Understanding stable levitation of superconductors from intermediate electromagnetics

A. Badía-Majós[a)]
Departamento de Física de la Materia Condensada-I.C.M.A., C.P.S.U.Z., María de Luna 1, E-50018 Zaragoza, Spain

(Received 15 February 2006; accepted 28 July 2006)

Levitation experiments with superconductors in the Meissner state are hindered by low stability except for specifically designed configurations. In contrast, magnetic force experiments with strongly pinned superconductors and permanent magnets display high stability, allowing the demonstration of striking effects, such as lateral or inverted levitation. These facts are explained by using a variational theory. Illustrations based on calculated magnetic field lines for various configurations are presented. They provide a qualitative physical understanding of the stability features.
[DOI: 10.1119/1.2338548]

I. INTRODUCTION

Levitation experiments based on the repulsive (or attractive) force between permanent magnets and superconductors are common. Almost everyone is fascinated and stimulated by the observation of floating objects. When the setup includes a high pinning (or high critical current) superconductor, the possibilities of lifting moderate weights and displaying lateral or inverted levitation are even more attractive. Recent developments of vehicles capable of supporting several passengers[1] have increased the interest in this topic.

As the number of levitation phenomena becomes larger, the difficulty of giving a reasonable explanation on how levitation works and giving a quantitative analysis has also increased. It is simple to understand that a magnet floating above a superconductor is related to flux expulsion and we may use the standard image technique in magnetostatics to make quantitative estimates. Specialized image models have also been introduced, which allow us to understand attractive forces.[2] However, such approximations are only useful for small displacements of tiny magnets close to the superconductor and do not include material parameters.

As an alternative and complementary point of view to previous work,[3] I will give a more general theoretical framework and a number of examples. The presentation is aimed at students who have had an intermediate course on electromagnetism and some background in classical mechanics. The main concepts involved are electromagnetic energy, thermodynamic reversibility and irreversibility, Lenz-Faraday's law of induction, and the use of variational principles. The presentation emphasizes the peculiarities of levitation with type-I and type-II superconductors. In both cases, the limitations imposed by Earnshaw's theorem,[4] which restricts levitation in electromagnetic systems, are avoided.[5]

II. BASIC SUPERCONDUCTIVITY AND VARIATIONAL PRINCIPLES

Superconductivity is a complex phenomenon, whose nature combines electromagnetic, thermodynamic, and quantum effects. For our purposes, the governing equations may be found from relatively simple considerations.

A. Type-I superconductors

We begin with the definition of the electric current density for conducting media

$$\mathbf{J} = nq\mathbf{v}, \tag{1}$$

where n is the volume density of the charge carriers, q their effective charge, and $\mathbf{v}$ their velocity. If the underlying material is such that charges can move without friction, Newton's second law gives

$$\frac{d\mathbf{J}}{dt} = \frac{nq^2}{m}\mathbf{E} \equiv \frac{1}{\mu_0\lambda^2}\mathbf{E}, \tag{2}$$

where λ defines a characteristic length, called the London penetration depth. Equation (2) leads to the property

$$\mathbf{E}\cdot\mathbf{J} = \mu_0\lambda^2\frac{d\mathbf{J}}{dt}\cdot\mathbf{J} = \frac{d}{dt}\left(\frac{\mu_0\lambda^2}{2}J^2\right). \tag{3}$$

If this relation is included in Poynting's theorem, it is apparent that the standard electromagnetic field energy is augmented by a new form of reversible storage, related to the kinetics of the moving charges. If we neglect the presence of electrostatic charges, we have the energy conservation law

$$\frac{d}{dt}\left(\int_{\mathbb{R}^3}\frac{B^2}{2\mu_0}dV + \int_{V_S}\frac{\lambda^2}{2\mu_0}|\nabla\times\mathbf{B}|^2dV\right) \equiv \frac{dU}{dt} = 0, \tag{4}$$

where V_S denotes the superconducting volume.

Because energy is conserved, the system will settle in some equilibrium configuration. If we use the field $\mathbf{B}$ as the independent variable and let δ denote derivatives with respect to it, we may express the equilibrium condition as the minimization of

$$U = \int_{\mathbb{R}^3}\frac{B^2}{2\mu_0}dV + \int_{V_S}\frac{\lambda^2}{2\mu_0}|\nabla\times\mathbf{B}|^2dV, \tag{5}$$

which implies that

$$\frac{\delta U}{\delta\mathbf{B}} = 0. \tag{6}$$

We minimize the quantity in Eq. (5) to obtain the static configuration for fixed sources (boundary conditions for the fields). Notice that this formulation reflects flux expulsion (diamagnetism) in superconductors, because B^2 is minimized. This expulsion is the Meissner state. The more conventional differential statement $\mathbf{B}+\lambda^2(\nabla\times\nabla\times\mathbf{B})=0$ (the London equation[6]) follows from the zero derivative condition Eq. (6).

B. Type-II superconductors

For certain superconducting materials, we need to relax the assumption that the electric current flow is completely free of losses. In the hard type-II superconductors only low (undercritical) currents are lossless. As a first approximation, we may assume lossless behavior for $J \leqslant J_c$ (J_c is the critical current for the material), and Ohm's law for $J > J_c$ as for normal metals [here $E=\rho_{\rm sc}(J-J_c)$]. The nature of such response of the charge carriers, including the interpretation of the intrinsic parameter J_c, may be found in Ref. 7. In brief, these materials can hold an internal magnetic flux as long as the field gradients (J) remain below a threshold. Above this value, the flux is unpinned and the underlying currents flow dissipatively.

I now show that the behavior of these materials also follows a variational law. Recall that the dynamical equations of a single particle under conservative forces may be obtained by a minimum action principle. That is the minimization of $\int L dt$ implies that

$$\frac{d}{dt}\left(\frac{\partial L}{\partial \dot{x}}\right)=\frac{\partial L}{\partial x}, \tag{7}$$

where $L=m\dot{x}^2/2-V$ is the Lagrangian. Note that nonconservative forces may not be treated variationally, so that Newton's second law is equivalent to

$$\frac{d}{dt}\left(\frac{\partial L}{\partial \dot{x}}\right)=\frac{\partial L}{\partial x}+F_{\rm ncons}. \tag{8}$$

Nevertheless, if we assume that $F_{\rm ncons}$ is a viscous drag force ($F_{\rm ncons}=-m\gamma\dot{x}$) with a friction constant γ, Eq. (8) may be obtained from minimizing $\int_0^{\Delta t}\hat{L}dt$:

$$\frac{d}{dt}\left(\frac{\partial \hat{L}}{\partial \dot{x}}\right)=\frac{\partial \hat{L}}{\partial x}. \tag{9}$$

We have defined $\hat{L}\equiv L+(m\gamma\dot{x}^2/2)t$, and assumed that $\Delta\dot{x} \ll \dot{x}$ for increments within the time interval $[0,\Delta t]$. Then Eq. (9) leads to $m\ddot{x}=-m\gamma\dot{x}-\partial V/\partial x$ as required.

The result (9) is a quasistationary variational principle, which may be applied in a time discretized description of the system (redefine $[0,\Delta t]$ and iterate).

Generalization is possible if we recall that for a single particle, $m\gamma\dot{x}^2$ is the energy loss per unit time. For instance, the eddy-current problem in normal (ohmic) metals may be solved iteratively by minimizing

$$S_n \equiv \int_0^{\Delta t}\int_{\mathbb{R}^3}\hat{\mathcal{L}}\,dV dt, \tag{10}$$

with $\hat{\mathcal{L}}\equiv B^2/2\mu_0+(\mathbf{E}\cdot\mathbf{J}/2)t$ as the modified Lagrangian density for the magnetostatic field. Recall that $\mathbf{E}\cdot\mathbf{J}$ corresponds to the energy dissipation per unit time and volume. Then, if we assume $\Delta E \ll E$ and use the stationary relations $\mathbf{E}=\rho\mathbf{J}$ and $\nabla\times\mathbf{B}=\mu_0\mathbf{J}$ in the time interval $[0,\Delta t]$, the minimization functional in Eq. (10) becomes

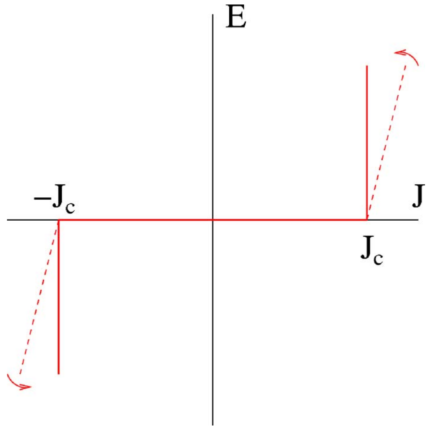

Fig. 1. $\{E,J\}$ graph (conduction law) for a hard type-II superconductor, according to Bean's model (Ref. 8). Vertical lines correspond to infinite resistivity above J_c.

$$F_n \equiv \int_{\mathbb{R}^3}\frac{(\Delta\mathbf{B})^2}{2\mu_0}dV+\int_{V_{\rm metal}}\frac{\rho\Delta t}{2\mu_0}|\nabla\times\mathbf{B}|^2 dV. \tag{11}$$

If we take variations with respect to the variable $\mathbf{B}$, we obtain $\delta F_n/\delta\mathbf{B}=0$, and

$$\frac{\Delta\mathbf{B}}{\Delta t}=-\nabla\times\left(\frac{\rho}{\mu_0}\nabla\times\mathbf{B}\right) \tag{12}$$

as expected. This equation in terms of increments is just the time-discretized version of Faraday's law ($\partial\mathbf{B}/\partial t=-\nabla\times\mathbf{E}$).

The application of the previous ideas to superconducting media follows naturally. We have to use a suitable form for the energy loss that is related to overcritical current flow. The simplest theory that accounts for losses in such conditions was proposed by Bean[8] in the context of magnetic hysteresis. In terms of a conduction law, Bean's model is equivalent to the $E(J)$ relation sketched in Fig. 1. Note that the multivalued graph corresponds to the overdamped limit of the physical properties mentioned previously: nondissipative current flow is allowed for current densities below a critical value J_c, and induced electric fields relate to the current density flow by an infinite slope resistivity. Obviously, the vertical relation is just an idealization of real cases in which there is a very high slope $\rho_{\rm sc}$. In terms of Eq. (10), Bean's law can be written as a quasistationary principle in which the modified Lagrangian is $\hat{\mathcal{L}}=\mathcal{L}+\mathcal{D}t$, with the dissipation function

$$\mathcal{D}=\begin{cases}0 & \text{if } J<J_c\\ \infty & \text{if } J>J_c.\end{cases} \tag{13}$$

The variational principle admits a simple treatment of this singular behavior. We may minimize the first term in Eq. (11) and replace the second one by the cutoff condition $J \leqslant J_c$.

By using a time discretization in layers of step size δt, that is, $t_n=n\delta t$, we obtain the following iterative model.[9] We minimize the quantity

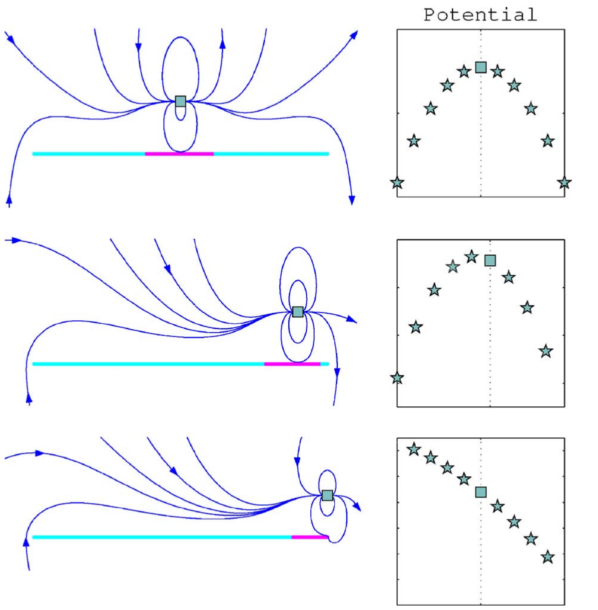

Fig. 2. Magnetic field lines around a horizontal magnetic dipole over a superconducting tape, for three positions of the magnet. Induced currents within the tape flow perpendicularly to the plot (outward within the small segment below the magnet, and inward for the rest). To the right, we plot the magnetostatic potential energy $U_m = -\mathbf{m}\cdot\mathbf{B}_S$ for small horizontal displacements of the magnet around each position.

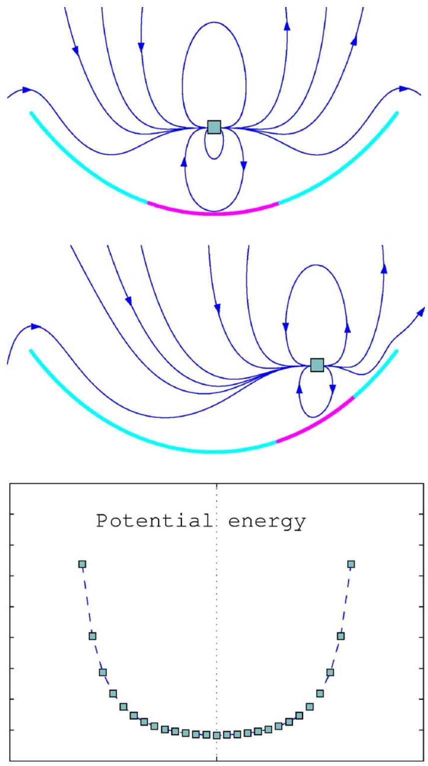

Fig. 3. Same as Fig. 2 for a superconducting tape with a concave section. The potential has been calculated for several positions around the plane of symmetry.

$$\frac{1}{2\mu_0}\int_{\mathbb{R}^3} |\mathbf{B}_{n+1} - \mathbf{B}_n|^2 \qquad (14)$$

with $|\nabla\times\mathbf{B}_{n+1}| \leq \mu_0 J_c$ for $V_S \subset \mathbb{R}^3$ and $\nabla\times\mathbf{B}_{n+1} = \mu_0 \mathbf{J}_{0,n+1}$ for $\mathbb{R}^3$ outside the superconductor V_S, where magnetic sources are located. Due to the inequality restriction on $\nabla\times\mathbf{B}_{n+1}$, a differential equation does not directly follow from the mathematical statement in Eq. (14). Another technical difficulty relates to the infinite domain for the integral. Thus, some transformations will be suggested for the practical application of the model (see Sec. IV).

However, from the physical point of view, the model is clearly linked to the compensation between minimum magnetic flux changes (Lenz-Faraday's law) and minimum energy losses in the evolution of the system.

III. LEVITATION IN THE MEISSNER STATE

Diamagnetism is a necessary condition for stability,[5] but is not sufficient. A specific geometrical configuration is required to produce a position of stable equilibrium in the presence of magnetic and gravitational fields. Thus, the radial force on a dipole magnet over a diamagnetic disk has been shown to be directed outward[10] unless the magnet is just above the center (where it vanishes). It is for this reason that Arkadiev[11] used a small permanent magnet that was floated over a concave lead bowl. Recall that lead is a type-I superconductor.

The relation between the geometrical arrangement and stability is illustrated in Figs. 2 and 3, where we display the structure of the magnetic field lines for a small horizontal magnet on top of a flat sample and on top of a curved one. In the first case, an arbitrarily small horizontal disturbance in the position of the magnet irreversibly leads to the magnet's fall over the edge. However, as seen in Fig. 3, the concave structure of the superconductor produces a restoring force that pulls the magnet back to its equilibrium position above the center.

The vertical force for horizontal configurations is repulsive, which can be seen by using the image method limit and considering the two poles of the magnet.

A. Minimum energy model

Arkadiev noted that levitation may be understood by the repulsive force between the real magnet and the corresponding magnetostatic image within the superconductor using the method of images.[11] Nevertheless, this method does not explain the aforementioned stability properties. The image is only simple for the limiting case of a superconducting half-space. Otherwise the problem becomes a nontrivial issue of complex variables on the flat disk[12] and may require much effort in arbitrary geometries. In the following we develop a theory including the fewest ingredients (see Sec. II) for studying the stabilization process in a general context. Figures 2 and 3 have been obtained as two specific applications.

We have solved the integral statement (5) by a numerical technique. Some modification of the model was helpful. For our purposes, the approximation ($\lambda \to 0$) may be used.[9] We minimize[13]

$$\frac{\mu_0}{2}\int_{\mathbb{R}^3} \mathbf{H}^2 dV \tag{15}$$

with $\nabla \times \mathbf{H} = \mathbf{J}_0$ outside the superconductor, and $\nabla \times \mathbf{H} = \mathbf{J}_S$ within. The first condition lets us include the magnetic sources, but numerical integration over $\mathbb{R}^3$ is not straightforward.

We now use vector differential calculus to restrict the infinite domain. Equation (15) is equivalent to the minimization of

$$\frac{\mu_0}{8\pi}\int\int_{VS} \frac{\mathbf{J}_S(\mathbf{x})\cdot \mathbf{J}_S(\mathbf{x}')}{|\mathbf{x}-\mathbf{x}'|} dV dV' + \int_{V_S} \mathbf{A}_0 \cdot \mathbf{J}_S dV, \tag{16}$$

where we have used $\mathbf{J}_S$ for the current density within the superconductor and $\mathbf{A}_0$ for the magnetic source vector potential.

If we can determine *a priori* (for example, by symmetry considerations) the current density streamlines (the paths of the charge carriers), a mutual inductance approach may be used. Equation (16) reduces to the minimization of

$$\frac{1}{2}\sum_{i,j} I_i M_{ij} I_j + \sum_i I_i A_{0i}. \tag{17}$$

Here the set of unknowns $\{I_i\}$ stands for the current elements flowing along appropriate circuits and M_{ij} is the mutual inductance matrix. The elements M_{ij} are geometric coupling coefficients between generic circuits C_i and C_j, which may be calculated if we make the substitution $\mathbf{J}_i dV \mapsto I_i d\mathbf{l}_i$. Then, we obtain the Neumann formula

$$M_{ij} = \frac{\mu_0}{4\pi}\oint_{C_i}\oint_{C_j} \frac{d\mathbf{l}_i \cdot d\mathbf{l}_j}{R_{ij}} = \frac{1}{I_i}\oint_{C_j} \mathbf{A}_i \cdot d\mathbf{l}_j, \tag{18}$$

where R_{ij} is the distance between points within the circuits C_i and C_j, and $\mathbf{A}_i$ is the vector potential created by the circuit C_i. Eventually, Eq. (17) becomes a series of linear equations in many variables that may be solved with moderate computational effort.

B. Application

To obtain Figs. 2 and 3 we have considered the magnetic field structure over a long flat/curved superconducting tape when a parallel dipole line is placed above and horizontally shifted. Recall that the dipole line vector potential is

$$\mathbf{A}_0 = \frac{\mu_0}{2\pi}\frac{\mathbf{m}\times \mathbf{r}}{r^2}, \tag{19}$$

where $\mathbf{m}$ is the magnetic moment per unit length. The superconducting current density will flow along parallel infinite straight lines given by

$$M_{ii} = \frac{\mu_0}{8\pi}, \tag{20a}$$

$$M_{ij} = \frac{\mu_0}{2\pi}\ln\frac{a^2}{(x_i - x_j)^2 + (y_i - y_j)^2}, \tag{20b}$$

where a is the radius of the wires, which are assumed to be equal, and along the z axis. These expressions have been obtained from Eq. (18) for parallel cylindrical wires and apply to the unit length.

IV. MAGNETIC LEVITATION WITH PINNED SUPERCONDUCTORS

With the advent of high T_c superconductivity, a number of exotic levitation configurations have been reported.[14,15] Today such experiments are routinely reproduced with the availability of good quality samples at liquid nitrogen temperatures. As was immediately recognized, the key property behind rigid (stable) levitation is the pinning of magnetic flux lines, which occurs within type-II superconductors such as high T_c superconductors.

A. Minimum action model

The stability issues in levitation experiments with type-II superconductors will be discussed within the framework introduced in Sec. II B. Thus, we have to solve the constrained minimization statement in Eq. (14).

As was discussed in Sec. III A, minimization is better realized when the problem is mapped onto the finite volume of the superconductor and we minimize:

$$\int\int_{V_S}\left[\frac{\mathbf{J}_{n+1}(\mathbf{x})\cdot \mathbf{J}_{n+1}(\mathbf{x}')}{|\mathbf{x}-\mathbf{x}'|} - 2\frac{\mathbf{J}_n(\mathbf{x})\cdot \mathbf{J}_{n+1}(\mathbf{x}')}{|\mathbf{x}-\mathbf{x}'|}\right] dV dV' + \frac{8\pi}{\mu_0}\int_{V_S} (\mathbf{A}_{0,n+1} - \mathbf{A}_{0,n})\cdot \mathbf{J}_{n+1} dV, \tag{21}$$

for $\mathbf{J}_{n+1} \leq J_c \in V_S$ and $\mathbf{A}_{0,n+1}$ given.

Again, minimization may be further discretized in spatial variables, and we obtain the mutual inductance formulation and minimization of

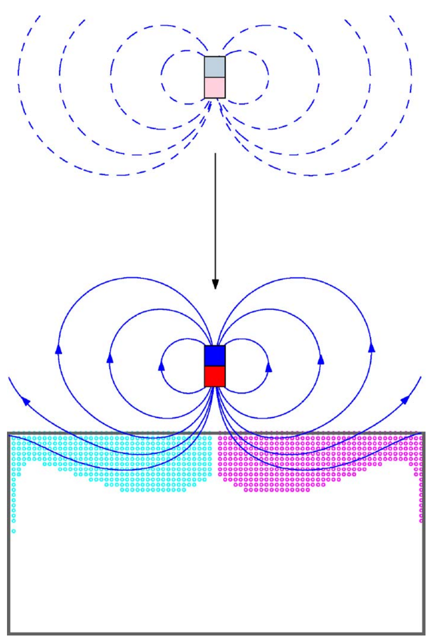

Fig. 4. A small magnet descends toward a cool superconductor, which rejects the magnetic field by means of critical currents with density $\pm J_c$. Induced current lines are perpendicular to the plot. Inward/outward flow is indicated by different shades for the right/left regions.

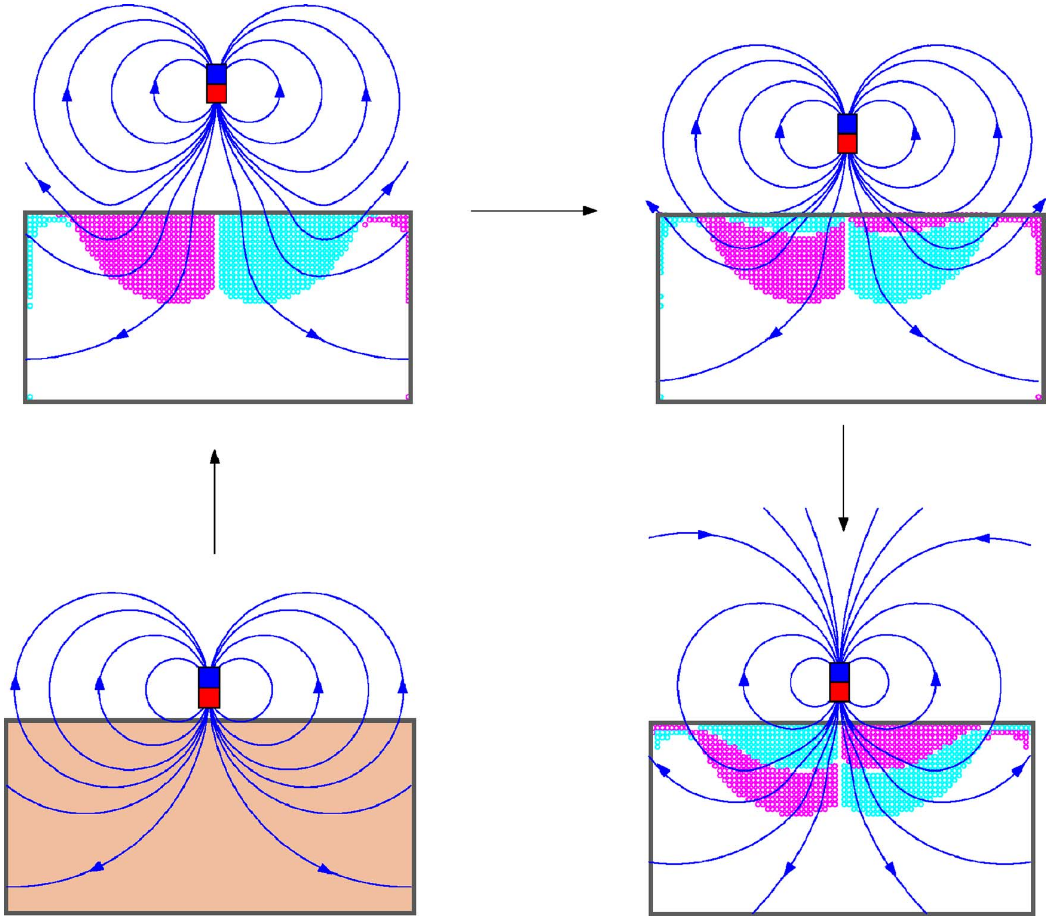

Fig. 5. Standard method for levitating a magnet above a hard superconductor. The superconductor is cooled with the magnet close to the surface (bottom-left picture), then the magnet is moved away and finally put back to its original position.

$$\frac{1}{2}\sum_{i,j} I_{i,n+1}M_{ij}I_{j,n+1} - \sum_{i,j} I_{i,n}M_{ij}I_{j,n+1} + \sum_{i} I_{i,n+1}(A_{0,n+1} - A_{0,n}) \tag{22}$$

for $|I_{i,n+1}| \leq I_c$ and $\mathbf{A}_{0,n+1}$ given.

This statement has to be solved as follows: we start from the initial configuration $\{I_{i,1}\}$ and iteratively find $\{I_{i,2}\},\{I_{i,3}\},\ldots$ in terms of the desired excitation process $\mathbf{A}_{0,1},\mathbf{A}_{0,2},\mathbf{A}_{0,3},\ldots$. In the following section we present some applications of statement (22) related to levitation configurations using magnets and superconductors. The interested reader is directed to Ref. 16 for the details on constrained numerical minimization. In brief, an augmented Lagrangian method, a generalization of the popular Lagrange multiplier technique in differential calculus, is used. Recall that the extrema of a function $f(\{x_i\})$ constrained by m relations of the type $\varphi_j(\{x_i\})=0$ are obtained by unconstrained minimization of

$$F(\{x_i\}) = f(\{x_i\}) + \sum_{j=1}^{m} \lambda_j \varphi_j(\{x_i\}) \tag{23}$$

with the additional unknowns λ_j (Lagrange multipliers). Specialized numerical methods allow us to add inequality constraints ($\psi_k(\{x_i\})<0, k=1,\ldots,p$, for instance) by minimizing functions of the kind

$$G(\{x_i\}) = f(\{x_i\}) - \sum_{k=1}^{p} \lambda_k s_k \log(s_k - \psi_k(\{x_i\})) + \sum_{j=1}^{m} \lambda_j \varphi_j(\{x_i\}) + \mu \sum_{j=1}^{m} \varphi_j(\{x_i\})^2, \tag{24}$$

where new auxiliary parameters s_k and μ have been introduced. Several numerical programs (both free[16] and commercial) are available, with excellent algorithms related to Eq. (24).

B. Examples

Most of the properties that are typically displayed in demonstrations with high T_c superconductors may be explained within the theory we have discussed. For instance, it is possible to describe the difference between cooling the superconductor close to the magnet or at a long distance. We can also predict the appearance of lateral restoring forces and calculate what happens when arbitrary displacements of the magnet occur around the superconductor.

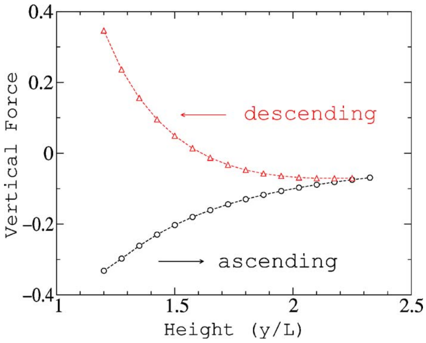

Fig. 6. Vertical force as a function of the normalized height for the small magnet in Fig. 5. A positive sign corresponds to repulsion, and a negative sign means attraction.

Figure 4 displays the magnetic field configuration which arises when a small magnet descends toward a cool superconductor. We consider a long superconducting bar (rectangular cross section $2W \times L$) and a magnetic dipole line on top. Notice that the magnetic field penetrates from the upper side, being excluded in the lower part of the sample. Superconducting currents along the infinite length of the bar with density $J = \pm J_c$ have been induced in the region penetrated by the field. The combination of induced currents and the dipole line produces the resultant magnetic field structure.

The repulsion between the magnet and the superconductor follows directly from the picture and the elementary force per unit volume $\mathbf{J} \times \mathbf{B}$. Orientation of $\mathbf{J}$ has to be done according to Lenz's law.

When the superconductor is cooled with the permanent magnet close to the surface, a new physical picture arises. The flux structure due to the magnet is frozen within the sample. The condition $\mathbf{J}_S = \nabla \times \mathbf{H} = 0$ is fulfilled, and no change occurs until the magnet is shifted. The reason for the passivity of the superconductor corresponds to the condition $E = 0$ in Fig. 1. However, if we move the magnet (see Fig. 5), an electric field arises ($\nabla \times \mathbf{E} = -\mu_0 \partial \mathbf{H} / \partial t$) and according to the $E(J)$ law, a critical current distribution appears.

In Fig. 5 we plot the simulation of a typical process of stable magnetic levitation. The magnet is initially moved away from the superconductor. Due to the Faraday-Lenz law, a current distribution appears, which tries to preserve the frozen flux lines. This current induces an attractive force due to the paramagnetic flux line structure, which is observed (the field is compressed toward the superconductor). However, if the movement of the magnet is reversed (rightmost part of Fig. 5), the new induced currents flow in the opposite direction to the previous structure because the sample is trying to avoid field penetration. As a consequence, the interaction force becomes repulsive and we can observe stable levitation. Figure 6 shows the actual behavior of the levitation force for a specific process. This force has been evaluated from the relation

$$\mathbf{F} = \int_{V_S} \mu_0 (\mathbf{H}_0 \times \mathbf{J}_S) dV, \tag{25}$$

which combines the magnetic force on moving charges and Newton's third law. $\mathbf{H}_0$ is the contribution to the field coming from the magnet.

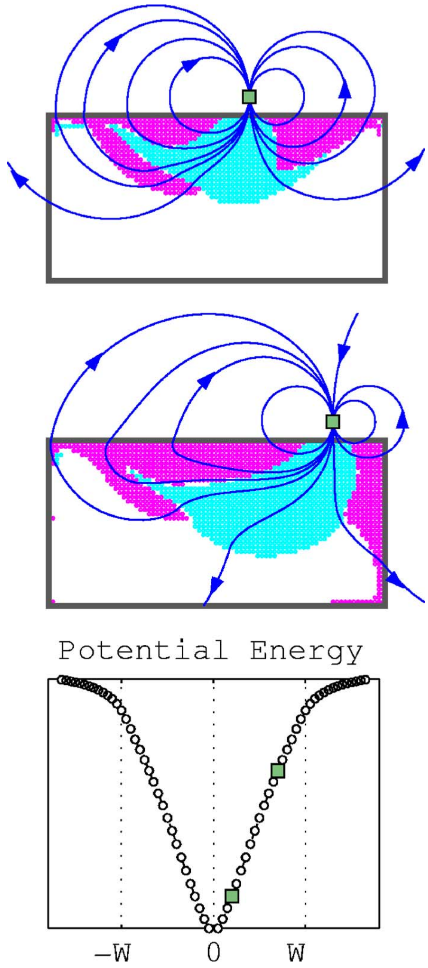

Fig. 7. Lateral displacement of the small magnet considered in Fig. 5. The restoring property is illustrated by the magnetostatic potential energy. W denotes the superconductor's half width. Large squares are used to indicate the corresponding positions of the magnet in the upper plots.

We can show that the process illustrated in Fig. 5 leads to a highly stable configuration. Figure 7 displays the current density and flux line structure that appear when the levitating magnet is laterally displaced. Again, the current density distribution preserves the flux line structure within the sample to the highest degree possible. As a consequence, a deep potential well in the magnetostatic energy U_m arises. We emphasize that the restoring force remains even when the magnet is beyond the edge of the superconductor. However, a noticeable change in the slope of U_m is observed.

V. CONCLUDING REMARKS

The main property of type-I superconductors is flux expulsion (diamagnetism). This phenomenon leads to a vertical repulsion force, which allows levitation. However, lateral stability is poor. Thus, magnets have to be levitated over bowl shaped superconductors. These facts follow from a minimum magnetostatic energy model. Further refinements such as the inclusion of finite penetration depth λ are easy to implement.

The basic ingredients underlying the rich phenomenology in levitation experiments with type-II superconductors are Faraday's law and a highly nonlinear $E(J)$ relation. When these properties are put in the form of a variational principle, the features of field or zero field cooling, finite size effects, and lateral stability are obtained directly. As in other physical systems (such as air cushions and eddy currents) lateral stability with hard type-II superconductors is achieved by a physical tendency to minimize the irreversible loss of energy. What is unusual in the case of superconductors is that dissipation occurs only during transitions between metastable states with different magnetic flux structures. Thus, as long as the levitating superconductor does not experience flux variations, energy must not be supplied.

VI. SUGGESTED PROBLEMS

(1) Show that the condition $\delta U/\delta\mathbf{B}=0$ in Eq. (5) leads to $\mathbf{B}+\lambda^2(\nabla\times\nabla\times\mathbf{B})=0$ within the superconductor. Hint: take the formal derivative of the integrand in the sense of a gradient. Derivatives with respect to $\mathbf{B}$ and (x,y,z) may be interchanged. Integration may be extended to $\mathbb{R}^3$ by taking $\lambda\rightarrow\infty$ outside the superconductor.

(2) Check that the statement (9) leads to the correct dynamical equations for an object falling in uniform gravity against a viscous force when $\Delta\dot{x}\ll\dot{x}$.

(3) Show that the time integration of Eq. (10), performed in the sense of averages over the interval $[0,\Delta t]$, leads to the spatial variational principle in Eq. (11).

(4) Show that Eq. (15) may be transformed into Eq. (16) by means of vector calculus manipulations. Hint: introduce the magnetic vector potential and use the divergence theorem.

(5) Obtain Eq. (20) and write a program for solving the matrix problem in Eq. (17). Apply it to different shapes of a superconductor.

ACKNOWLEDGMENTS

I am indebted to L. A. Angurel and M. Mora for assistance with levitation experiments and useful discussions. Financial support from Spanish CICyT under Project No. MAT2005-06279-C03-01 is acknowledged.

[a]Electronic mail: anabadia@unizar.es

[1] J. Wang *et al.*, "The first man-loading high temperature superconducting Maglev test in the world," Physica C **378–381**, 809–814 (2002).
[2] A. A. Kordyuk, "Magnetic levitation for hard superconductors," J. Appl. Phys. **83**, 610–612 (1998).
[3] E. H. Brandt, "Rigid levitation and suspension of high-temperature superconductors by magnets," Am. J. Phys. **58**, 43–49 (1990).
[4] S. Earnshaw, "On the nature of the molecular forces which regulate the constitution of the luminiferous ether," Trans. Cambridge Philos. Soc. **7**, 97–112 (1842).
[5] M. D. Simon, L. O. Heflinger, and A. K. Heim, "Diamagnetically stabilized magnet levitation," Am. J. Phys. **69**, 702–713 (2001).
[6] R. Feynman, R. B. Leighton, and M. Sands, *The Feynman Lectures on Physics* (Addison-Wesley, Reading, MA, 1965), Vol. 3.
[7] M. Tinkham, *Introduction to Superconductivity* (McGraw-Hill, New York, 1996), 2nd ed.
[8] C. P. Bean, "Magnetization of high-field superconductors," Rev. Mod. Phys. **36**, 31–39 (1964).
[9] In most experimental conditions, the kinetic energy of the charge carriers may be neglected because λ (submicron range) is much smaller than the scale of the sample (centimeters).
[10] L. C. Davis, E. M. Logothetis, and R. E. Soltis, "Stability of magnets levitated above superconductors," J. Appl. Phys. **64**, 4212–4218 (1988).
[11] V. Arkadiev, "A floating magnet," Nature (London) **160**, 330 (1947).
[12] L. C. Davis and J. R. Reitz, "Solution to potential problems near a conducting semi-infinite sheet or conducting disk," Am. J. Phys. **39**, 1255–1265 (1971).
[13] In this work, we follow the convention for macroscopic fields: $\nabla\times\mathbf{B}=\nabla\times(\mu_0\mathbf{H})=\mu_0(\mathbf{J}_S+\mathbf{J}_0)$ and $\nabla\cdot\mathbf{B}=\nabla\cdot(\mu_0\mathbf{H})=0$, that is, superconducting carriers are treated as free charges with flow density $\mathbf{J}_S$.
[14] F. Hellman, E. M. Gyorgy, D. W. Johnson, Jr., H. M. O'Bryan, and R. C. Sherwood, "Levitation of a magnet over a flat type-II superconductor," J. Appl. Phys. **63**, 447–450 (1988).
[15] W. G. Harter, A. M. Hermann, and Z. Z. Sheng, "Levitation effects involving high T_c thallium based superconductors," Appl. Phys. Lett. **53**, 1119–1121 (1988).
[16] A. R. Conn, N. I. M. Gould, and Ph. L. Toint, *LANCELOT: A Fortran Package for Large-Scale Nonlinear Optimization* (Springer-Verlag, Berlin, 1992).